International Journal of Pharmaceutics 433 (2012) 71–78

Contents lists available at SciVerse ScienceDirect

International Journal of Pharmaceutics

journal homepage: www.elsevier.com/locate/ijpharm

Miscibility analysis of particulate solid dispersions prepared by electrospray deposition

Kohsaku Kawakami*

National Institute for Materials Science, International Center for Materials Nanoarchitectonics (MANA), Biomaterials Unit, 1-1 Namiki, Tsukuba, Ibaraki 305-0044, Japan

ARTICLE INFO

Article history:
Received 17 February 2012
Accepted 30 April 2012
Available online 11 May 2012

Keywords:
Electrospray deposition
Solid dispersion
Amorphous
Miscibility
Thermal analysis

ABSTRACT

Physical characteristics of solid dispersions were investigated using carbamazepine (CBZ) and prednisolone (PDN) as model drugs, and poly(vinyl pyrrolidone) and Eudragit as polymeric excipients. Electrospray method provided particulate formulations, of which the particle size was typically in the order of micrometers, when the polymer concentration of the solution used for the preparation was below 2% (w/v). Decrease of the solution concentration and flow rate resulted in a decrease in the particle diameter, as theoretically expected. Also, the particle size could be reduced to 400 nm by increasing the conductivity of the solution by the addition of salts. When poly(vinyl pyrrolidone) K90 was used as an excipient, CBZ was homogeneously loaded up to ca. 40%, and if a greater amount was added, the excess CBZ was separated as a pure crystalline phase. PDN was homogeneously loaded up to ca. 60%. However, in contrast to CBZ, excess PDN maintained the amorphous state, even when a greater amount was added. The separated excess PDN phase was crystallized in the heating process during thermal analysis. In addition to the thermodynamic factor, there seems to be a dynamic factor to separate drug phase from the excipient phase, depending on their molecular weight and miscibility during the electrospray deposition process. The mechanism for particle formation by electrospray deposition is discussed with emphasis on the miscibility between drug and excipient.

1. Introduction

Amorphization is one of the important formulation technologies in the pharmaceutical industry (Serajuddin, 1999; Kawakami, 2009, 2012). Although it can be regarded as a conventional technology for injectable freeze-dried (FD) formulations, the number of the marketed oral amorphous formulations is still limited due to problems including its physical and chemical instability. Notably, the lack of a protocol to predict physical stability, i.e., crystallization rate, is a serious issue that inhibits the wide use of the amorphization technology for oral drug delivery (Bhugra and Pikal, 2008; Kawakami, 2009). In the case of injectable formulations, storage under refrigerated conditions is relatively acceptable, because the formulations are typically handled in hospitals. On the other hand, oral formulations are frequently handled by patients themselves. In this case, storage in the refrigerator is not a favorable option, so that the stability requirement for the oral formulation can be more severe. The higher energy state of the amorphous material means that its chemical reactivity is higher than the crystalline form (Byrn et al., 2001). This may be improved by various technologies, including intentional annealing to decrease the molecular mobility (Luthra et al., 2008); however, the stability problem still be a valid reason to cease application of amorphous dosage forms. Thus, further understanding on physical chemistry of amorphous formulations is required for their effective use.

Another challenge for amorphous formulations is that special manufacturing facilities are required for production. There are various manufacturing methodologies available, most of which require solvents during processing (Kawakami, 2012). Because drugs for oral delivery that require amorphous technology are not soluble in water, the manufacturing facilities must be operated with organic solvents. If flammable solvents are used during manufacture, investment on facilities increases significantly. Therefore, solvent-free manufacturing technologies, such as hot melt extrusion, have been significant interest recently (Breitenbach, 2002; Guns et al., 2011). Also, another problem in amorphous production methods is that the drug molecules are usually subjected to high temperatures that may degrade the active pharmaceutical ingredients.

Electrospray deposition (ESD) is a novel versatile technique that has been applied to micro/nanofabrication of various materials including pharmaceutical products (Chakraborty et al., 2009; Zhang and Kawakami, 2010; Zhang et al., 2011). In this technology, a high voltage is applied to the solution that contains the drug and excipients. Solutions are dispersed into fine droplets, due to coulombic repulsion between the ions near the solution surface.

* Tel.: +81 29 860 4424; fax: +81 29 860 4708.
E-mail address: kawakami.kohsaku@nims.go.jp

0378-5173/$ – see front matter © 2012 Elsevier B.V. All rights reserved.
http://dx.doi.org/10.1016/j.ijpharm.2012.04.082

The fine droplets quickly lose the solvents and the residual solutes are accumulated on the targets as fine particles. Various characteristics, including sustained release and enhanced dissolution rate, are expected for ESD particles, depending on the morphology of the formulation and the characteristics of the excipients used. In addition to the ability for nanofabrication, the ESD method can also be regarded as an amorphization technique. Thus, the electrospray formulation is expected to improve the dissolution of poorly water-soluble drugs by two mechanisms; nanosizing and amorphization. The notable advantage of this method is that it can be operated under ambient temperature and pressure conditions. In our previous study, the effect of various solution and processing parameters on the particle morphology/formation was clarified (Zhang and Kawakami, 2010). Also, a coaxial nozzle was used to prepare core–shell type amorphous particulate formulations, by which oral absorption of a poorly soluble drug, griseofulvin, was significantly improved (Zhang et al., 2011). In this study, bulk amount of formulations were prepared for investigating their physical characteristics by increasing the nozzle numbers. The capability of this formulation technology to prepare particulate amorphous formulations is discussed with emphasis on the miscibility of each component.

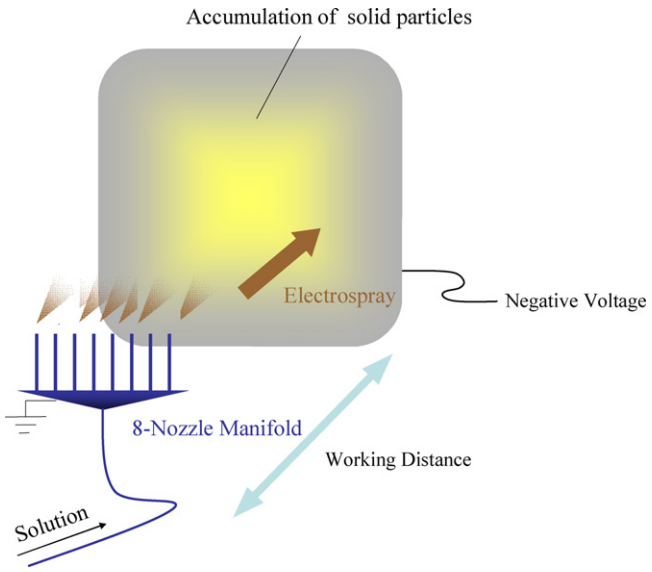

Fig. 1. Schematic representation of the electrospray apparatus.

2. Materials and methods

2.1. Materials

Poly(vinyl pyrrolidone) (PVP) K30, K90, and carbamazepine (CBZ) were obtained from Wako Pure Chemicals (Osaka, Japan). PVP K12 and prednisolone (PDN) were purchased from Sigma–Aldrich (St. Louis, USA) and Nacalai Tesque (Kyoto, Japan), respectively. Poly(butyl methacrylate-co-(2-dimethylaminoethyl) methacrylate-co-methylmethacrylate), which is commonly called as Eudragit E-100, were obtained from Rohm Pharma GmbH (Darmstadt, Germany). All reagents were used as supplied.

2.2. Electrospray deposition

Ethanol solutions of polymer and drug were supplied using a syringe pump, at a flow rate of 5 mL/h unless otherwise mentioned, to a nozzle branched into eight stainless-steel needles with ca. 1 cm intervals, each of which has the diameter of ca. 1 mm. An aluminum plate deposition target was placed parallel to the nozzle, which was facing upward to ensure homogeneous distribution of solution to each needle, as shown schematically in Fig. 1. A high negative voltage (−25 kV) was applied to the target and the nozzle was grounded. The working distance from the nozzle to the target was 15 cm. All preparations were carried out in an acrylic chamber at room temperature. The humidity of the chamber was controlled to lower than 20%RH by flowing nitrogen gas. The residual solvent in all preparations was below the detection level (0.1%) according to thermogravimetry analysis coupled with gas analysis using mass spectrometry. At least two formulations were prepared for each composition for assuring reproducibility.

2.3. Freeze-drying

FD formulations were prepared using an AsOne FDU-12AS apparatus (AsOne, Osaka, Japan) to obtain information regarding the miscibility between PVP K90 and the drugs. Both drug and PVP K90 were dissolved in *t*-butanol at 40 °C at a total concentration of ca. 2% (w/v), followed by rapid freezing in a cell at −20 °C. The frozen solution was subjected to the vacuum at room temperature for 3 h. The temperature was subsequently raised to 40 °C and held for 30 min to remove residual solvent. The dried cakes were stored in the refrigerator before use.

2.4. Differential scanning calorimetry (DSC)

DSC measurements were performed on DSC Q2000 (TA Instruments, New Castle, USA), which is periodically calibrated using indium and sapphire. Approximately 5 mg of sample was pressed into a disk shape and subjected to measurement in a sealed aluminum pan with pinholes. Dry nitrogen was used as the inert gas at a flow rate of 50 mL/min. Measurements were done in at least duplicate to ensure reproducibility. PVP–PDN formulations were investigated in the modulated-temperature mode, in which the samples were heated at 2 °C/min with a 60 s period and 0.5 °C amplitude.

2.5. X-ray powder diffraction (XRPD)

XRPD patterns were acquired on a Rigaku RINT Ultima X-ray diffraction system (Rigaku Denki, Tokyo, Japan) using CuKα radiation. The voltage and the current were 40 kV and 40 mA, respectively. Data were collected between 5° and 40° (2 theta) at intervals of 0.02° with a scan speed of 2°/min. Although no XRPD data are presented in this paper, all the formulations exhibited consistent results in terms of diffraction patterns and intensity with the DSC measurements.

2.6. Particle morphology

Particle morphology was investigated using scanning electron microscopy (SEM) (S4800, Hitachi, Tokyo, Japan) with an accelerating voltage of 5 kV. Samples were sputter-coated using a platinum coater (E-1030 ion sputter, Hitachi, Tokyo, Japan) before measurements. Particle size was determined by SEM image analysis using Mac View ver. 4.0 (Mountech, Tokyo, Japan). Three hundred particles were randomly selected from an image to obtain the Heywood diameter. Volume-mean diameter was used for the analysis.

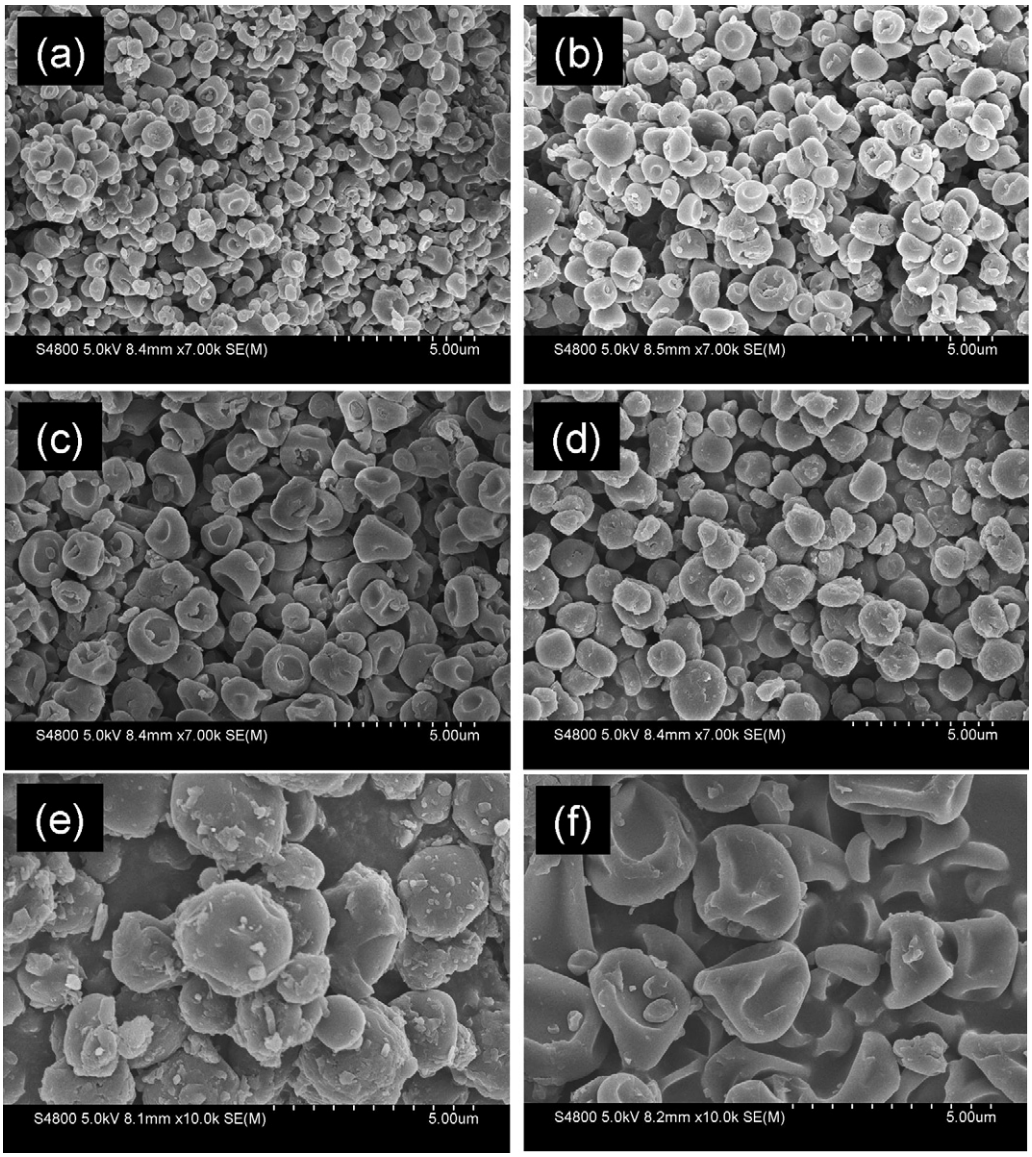

Fig. 2. SEM images of ESD particles. The solutions and flow rates used were (a) 1% (w/v) PVP K30, 1 mL/h, (b) 1% (w/v) PVP K30, 4 mL/h, (c) 1% (w/v) PVP K30, 6 mL/h, (d) 1% (w/v) PVP K30 + 1% (w/v) CBZ, 1 mL/h, (e) 1% (w/v) PVP K30 + 2% (w/v) CBZ, 5 mL/h, (f) 1% (w/v) PVP K30 + 2% (w/v) PDN, 5 mL/h.

2.7. Solution conductivity

Solution conductivity was measured using a conductivity cell attached to an Orion benchtop multimeter (Thermo Fisher Scientific, Waltham, USA).

3. Results and discussion

3.1. Effect of operating conditions on formulation morphology

Our previous investigation using a single nozzle apparatus revealed that the solution flow rate had a significant influence on the particle size, while other parameters such as the nozzle diameter and strength of the electric field were less significant (Zhang and Kawakami, 2010). The same conclusion was derived in the scale-up system used in this study. The insignificance of the nozzle diameter is a reasonable observation, because the size of the droplets produced from the top of a Taylor-cone, is much smaller than the nozzle diameter. The nozzle diameter would only have some effect, if it is sufficiently small enough to affect shape of the Taylor-cone.

The particulate formulation could be obtained when the concentration of polymeric excipients was below 2% (w/v) for PVP and Eudragit. A fibrous structure was obtained at higher concentrations. Fig. 2 shows SEM images of ESD particles for some representative compositions. The particles in (a)–(c) were produced from 1% (w/v) PVP K30 ethanol solution with various flow rates. Each particle has cavities on the surface, which is a typical shape of polymeric particles produced by drying droplets (Vehring, 2008; Kawakami et al., 2010). The shape is explained by a concentration gradient, i.e., accumulation of the polymer molecules on the surface region due to slow diffusion during the drying process (De Gennes, 2002; Okuzono et al., 2006) followed by the formation of hollow particles after removal of the solvent, which can deform easily due to low integrity of the particle skin. The particle size increased with the flow rate as expected from the scaling law shown later. The PVP K30 particles with CBZ shown in (d) have lost the cavity structure. Thus, CBZ is expected to fill the interior of the particles to prevent deformation during drying. Also, an increase in the particle size was observed as the total concentration increased. The effect of drug addition on the particle morphology is likely to be dependent on the drug type. (e) and (f) PVP particles in which double amounts of

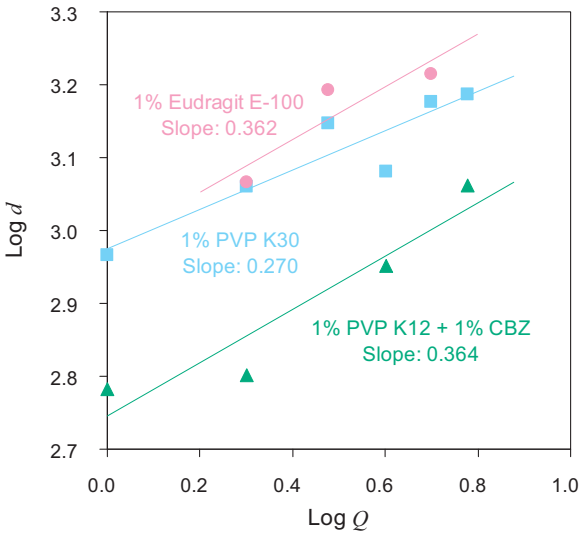

Fig. 3. Particle size (nm) of ESD formulations as a function of the flow rate, Q (mL/h). The solutions used are indicated in the figure.

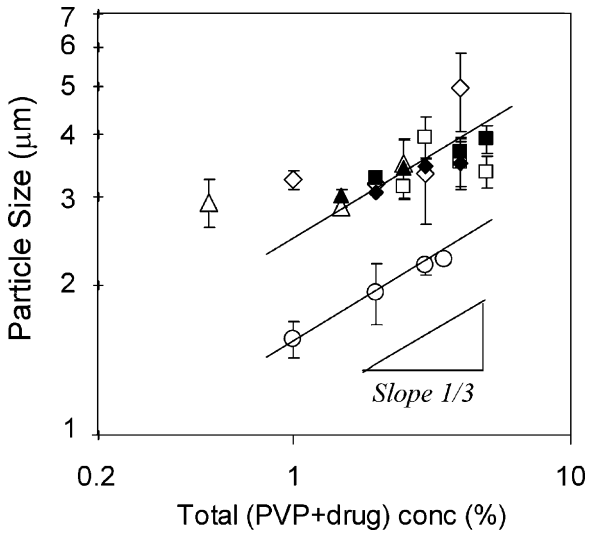

Fig. 4. Particle size of ESD formulations as a function of the total solute concentration. Each data is shown as mean value (n = 2 or 3) with standard deviations as error bars. △: 0.5% (w/v) PVP K90 + CBZ, ◇: 1% (w/v) PVP K90 + CBZ, □: 2% (w/v) PVP K90 + CBZ, ▲: 0.5 (w/v) PVP K90 + PDN, ♦: 1 (w/v) PVP K90 + PDN, ■: 2% (w/v) PVP K90 + PDN, ○: 1% (w/v) PVP K30 + CBZ. The solid lines have a slope of 1/3.

CBZ or PDN were loaded. Again, the particle shape became spherical with the addition of CBZ. The small prismatic fragments are considered to be CBZ crystals, because the amount of CBZ exceeds the loading limit in this ratio, as shown later. However, the caved structure was maintained with the addition of the same amount of PDN, which suggests a difference in the behavior of the PDN molecules from that of CBZ. The solubility of PDN in ethanol is lower than that of CBZ; therefore, PDN may crush out promptly during the drying process, resulting in the accumulation of precipitates on the surface regions of the droplets. Also, the interaction between PDN and PVP may be stronger than that with CBZ as shown later in the DSC studies which would lead to a partial distribution of PDN in the surface region.

Fig. 3 shows the effect of flow rate on the mean particle diameter for some representative compositions. If homogeneous spherical particles are formed, the particle diameter d should follow the scaling law shown below (Ganán-Calvo et al., 1997; Zhang and Kawakami, 2010).

$$d \propto Q^{1/3}, \tag{1}$$

where Q is the flow rate of the feed solution. In the case of ESD particles without drug molecules, this equation should be a very rough approximation, due to the hollow structure. However, although there were some deviations, the slopes of the plot were around 1/3, regardless of the presence of drug molecules. Thus, the particle size appears to approximately obey the scaling law for the flow rate, even in the scale-up system.

Fig. 4 summarizes the effects of solution concentration on the particle size. Given that one particle was formed from one droplet, the diameter of the particle, d, can be calculated using the diameter of a droplet, D.

$$d = D\left(\frac{\rho_d}{\rho_p}C\right)^{1/3} \tag{2}$$

where ρ_d and ρ_p are the densities of the droplet and the particle, respectively. ρ_d is almost unity at ambient temperature. C is the fraction of solute in the droplet, that is, the concentration (w/w). As can be seen in the figure, when the same polymeric material (PVP K90) was used, the particle size could roughly be regarded as a function of the total solute concentration regardless of the drug type, except that the drug-free particles were larger than expected. This should be because the drug-free polymeric particles have hollow structure. The fitting line had a slope of ca. 1/3, which corresponds with the expectation from Eq. (2). A change in the polymer grade provided a different line, but the slope was also 1/3. The particle size decreased with decreasing molecular weight of PVP, probably due to the decrease in the solution viscosity (Zhang and Kawakami, 2010).

3.2. Control of the particle size by dependency on the solution conductivity

Smaller particles can be prepared by controlling various factors, including the flow rate, solute concentration, viscosity, and conductivity. However, the former two options are not favorable, because they decrease the production rate. Although viscosity can be lowered by decreasing the solute concentration, it also decreases the production rate. Replacement of solvent is another option to lower viscosity; however, its effect is not straightforward because it also affects other solution parameters significantly. Thus, the simplest way to decrease viscosity is to change the conductivity (Zhang and Kawakami, 2010), which can be done by a small change in the solvent composition without affecting other solution parameters significantly. A small amount of water or sodium chloride solutions were added to ethanol to control the conductivity. Fig. 5 shows the effect of conductivity on the particle size, in which the size decreased as a function of the conductivity. The size decreased from ca. 1600 nm to ca. 400 nm by adding 10% (v/v) of 0.2 M sodium chloride solution. Thus, it was demonstrated that micrometer-order particles can be easily transformed to nanoparticles by simply adding a small amount of salt solution.

3.3. Miscibility between PVP K90 and CBZ

Miscibility between PVP K90 and the model drugs was investigated for formulations prepared by two different methods, FD and ESD. Fig. 6 shows DSC curves for the PVP/CBZ formulations prepared by both methods. The only thermal event observed for the FD formulations were large endothermic peaks at around 80 °C (Fig. 6(a)), when the amount of CBZ was below PVP/CBZ = 6/4, which could be elucidated as dehydration endotherms. Note that no residual t-butanol was detected by thermogravimetric-mass spectrometry analysis (data not shown). No melting endotherms were evident

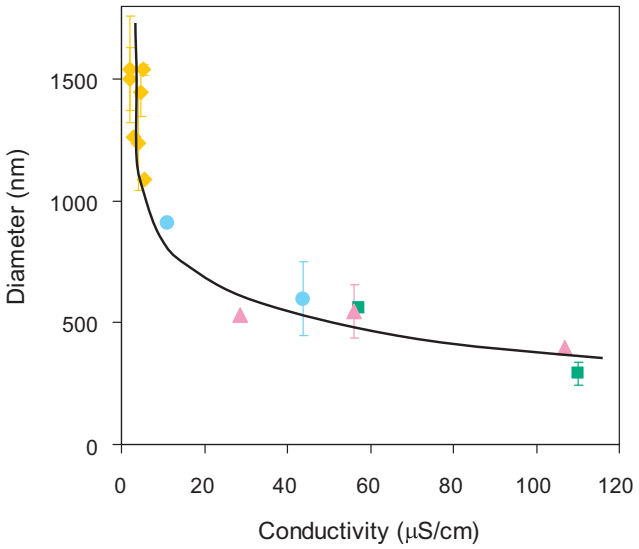

Fig. 5. Particle size of ESD formulations as a function of solution conductivity. Diamonds indicate particles obtained using ethanol aqueous solutions with 1% (w/v) PVP K30. The amount of water was 0%, 5%, 10%, 15%, 20%, 30%, 40% (v/v), and the conductivity was increased in this order. Circles represent particles obtained by the addition of 2% or 10% (v/v) of 0.05 M sodium chloride solution to the PVP K30 ethanol solution. The final PVP concentration was 1% (w/v). In the same manner, 0.1 M and 0.2 M sodium chloride solutions were added at 5%, 10%, 20% (v/v) and 5%, 10% (v/v), respectively, to the PVP solution, and the data are shown by triangles and squares, respectively. Each data is shown as mean value ($n = 2$) with standard deviations as error bars. The points that do not have error bars mean that the bars are shorter than the symbol size.

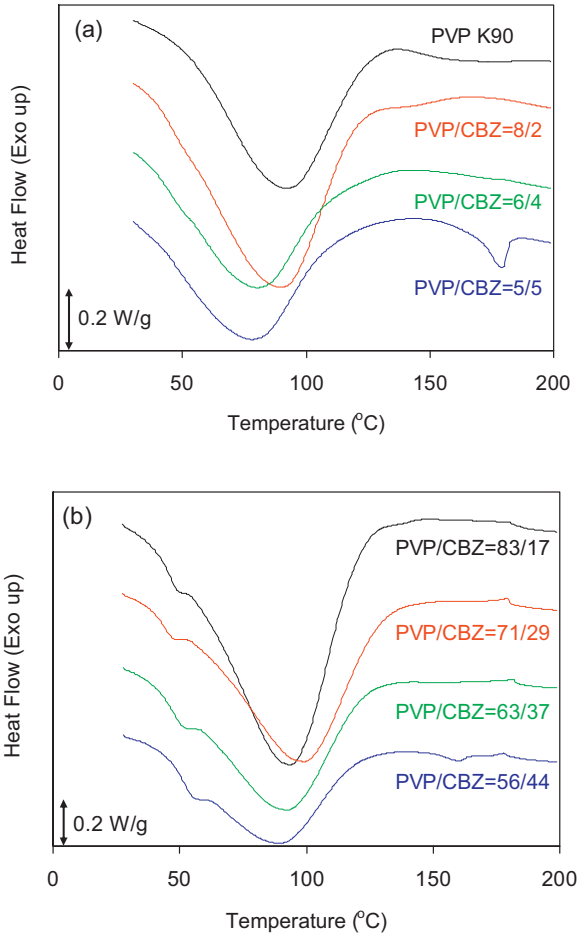

Fig. 6. DSC curves of (a) FD and (b) ESD formulations prepared using PVP K90 and CBZ. The mixing ratios are presented in the figure.

when the amount of CBZ was below PVP/CBZ = 6/4, so that glass transition temperatures should be found in the heating process; however, it is most likely that the glass transition temperatures are obscured by the dehydration peak. When the amount of CBZ was larger than PVP/CBZ = 6/4, a small endotherm was observed at around 165 °C, which could be attributed to the melting of form III of CBZ. XRPD observation also revealed the presence of a small amount of the form III in the formulation (data not shown). Although recrystallization into form I usually follows after the melting of the form III (Grzesiak et al., 2003; Kawakami, 2010), this was not observed for these formulations, presumably due to inhibition by the excipient. Fig. 6(b) shows DSC curves of the ESD formulations. Unlike the FD samples, there were shoulders on the low-temperature side of the dehydration peaks, and the glass transition behavior was observed at around 175–180 °C, which coincides with the glass transition temperature of PVP K90, and thus an almost pure PVP phase seemed to be separated for ESD samples. No residual solvent was found for the ESD samples, as with the FD samples. Thus, the shoulders on the low-temperature side of the dehydration endotherms seem to be due to the glass transition of a mixed phase. The onset temperatures of this event were almost constant at 40 °C, which suggests that there was a phase separation into almost pure PVP and the mixed phases in the ESD formulations, regardless of the mixing ratio. This is not surprising, because the components in a droplet tend to be separated during the drying process according to their molecular weight (Vehring, 2008; Kawakami et al., 2010). In other words, in the quick drying process of ESD, CBZ is likely to diffuse rapidly enough to follow the shrinkage of the droplets, while this is not the case for PVP, which results in the accumulation of PVP on the particle surface. The glass transition temperature of the mixed phase is lower than those of PVP and CBZ (61 °C, Baird et al., 2010), which may be explained by inclusion of water molecules. The loading limit of CBZ in the amorphous state was almost identical at 40% for both preparation methods, although the mixing state appeared to be different.

Fig. 7 shows the DSC curves of the second scan for the PVP/CBZ formulations, after heating up to 200 °C. In this case, only one glass transition temperature, which could be attributed to the mixed phase, was observed for both preparation methods. Thus, a well-mixed state was obtained by heating up to 200 °C. This was also the case for samples in which the crystalline CBZ phase was present in the initial state. Thus, the crystalline CBZ phase seems to be dispersed homogeneously in the PVP/CBZ phase after melting. The glass transition temperatures of the mixed phase are summarized in Fig. 8. The glass transition temperatures of the formulations prepared by both methods fall on the same curve, which indicates that the history of the formulations totally disappeared by heat treatment. A line based on the Gordon–Taylor equation is also shown, which was higher than the experimental values. Thus, the mixing state of PVP and CBZ was not thermodynamically ideal and the interaction between the components and their molecular volume appeared to have an influence on the glass transition behavior.

The heating of PVP/CBZ formulations up to 200 °C always provided homogeneous structures, regardless of the preparation method; therefore the stop temperature of the first scan was decreased to 140 °C in the subsequent study. In this case, crystalline CBZ phase and an almost pure PVP phase, of which the glass transition temperature was higher than 140 °C, were maintained as they were; however, removal of the solvent enabled observation of the glass transition behavior of the mixed phase in the second scan, as shown as Fig. 9. The glass transition behavior of FD samples when the CBZ content was below PVP/CBZ = 6/4 coincided with those after heating up to 200 °C. However, this procedure enabled the observation of the glass transition of the mixed phase above that ratio, because the crystalline CBZ was maintained in the first scan. The glass transition temperature of PVP/CBZ = 6/4 agreed well

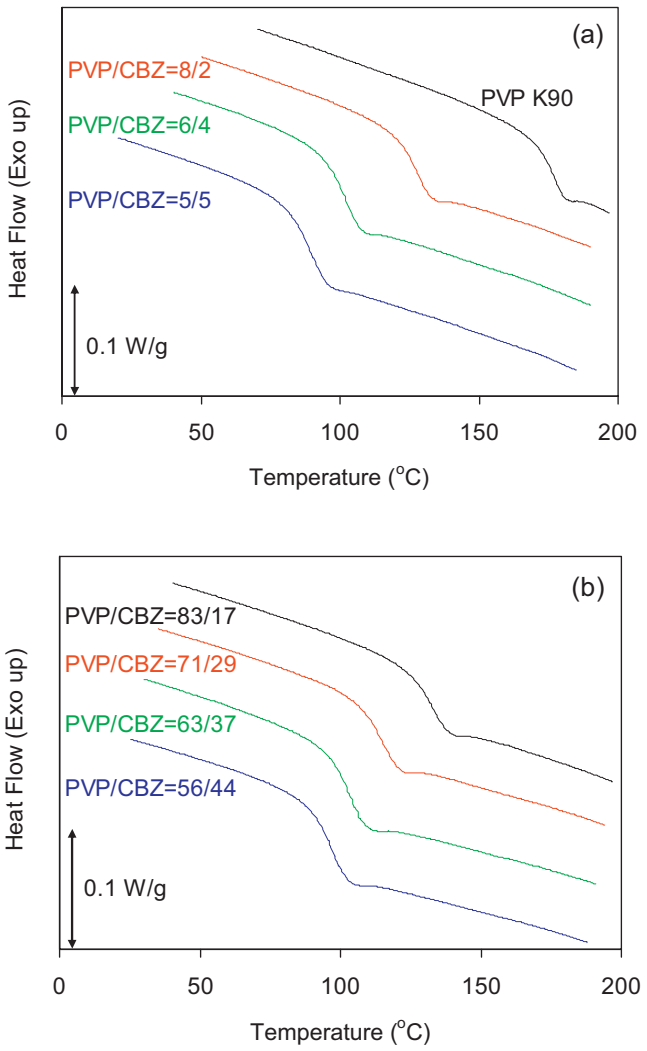

Fig. 7. The 2nd DSC scan of (a) FD and (b) ESD formulations prepared using PVP K90 and CBZ. The mixing ratios are presented in the figure. The measurements were done after heating the sample up to 200 °C at 10 °C/min.

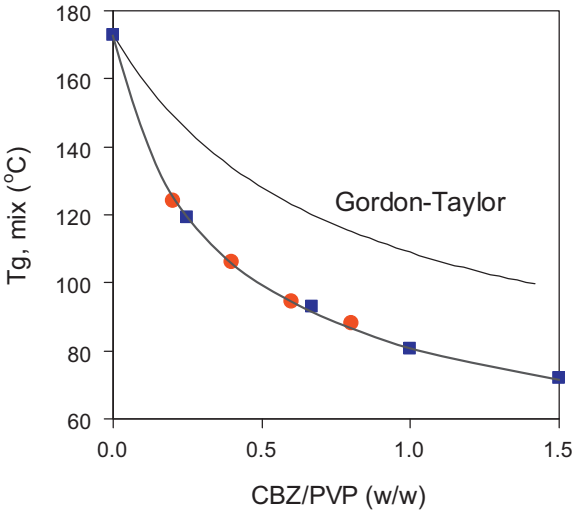

Fig. 8. Glass transition temperatures of PVP/CBZ formulations in the 2nd scan (Fig. 7). ● : FD and ■ : ESD formulations. The expected glass transition temperature from the Gordon–Taylor equation is presented as a thin line, and was higher than the experimental data.

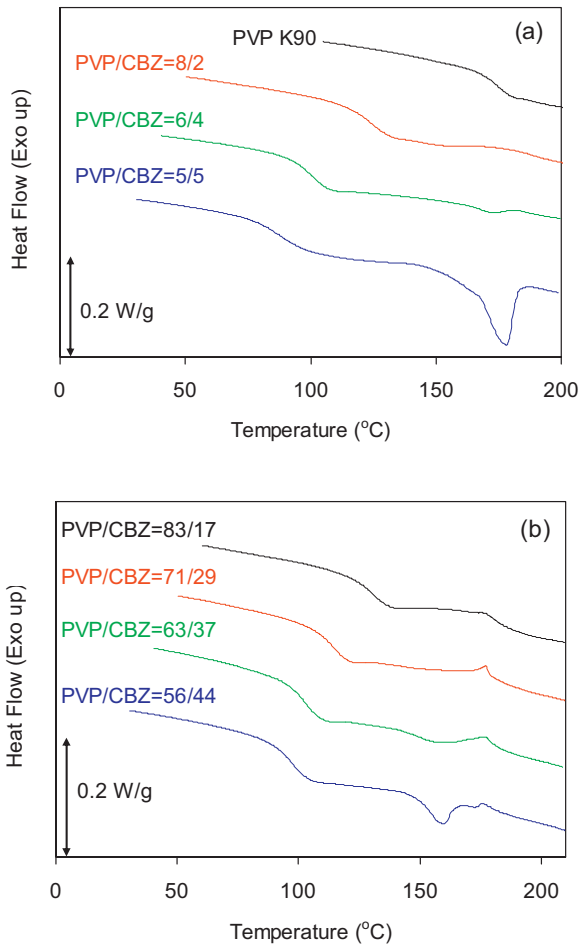

Fig. 9. The 2nd DSC scan of (a) FD and (b) ESD formulations prepared using PVP K90 and CBZ. The mixing ratios are presented in the figure. The measurements were done after heating the sample up to 140 °C at 10 °C/min.

with that of the mixed phase of PVP/CBZ = 5/5, and further increase in the CBZ content also provided the same glass transition temperature (data not shown), which suggests that the solubility of CBZ in the PVP matrix can be regarded as ca. 40%. For the ESD samples, the glass transition temperature that can be assigned to the pure PVP phase was present in all the formulations, which indicates that phase separation was more distinct for the ESD formulations. However, it was also true that the glass transition temperature of the mixed phase approximately corresponded with those of the mixed phases of the FD formulations, which suggests that the difference between the FD and ESD formulations, at least after thermal treatment at 140 °C, is the slight separation of a pure PVP phase, probably in the surface region of the particles. These observations clearly indicate difference in the mixing state between the FD and ESD formulations.

3.4. Miscibility between PVP K90 and PDN

In the case of CBZ, excess CBZ that was not solubilized in the PVP matrix, was present as the crystalline phase. However, PVP/PDN formulations were always in the amorphous state even at PVP/PDN = 25/75, and the excess PDN was crystallized during the heating process of the DSC measurement. The loading limit at which crystallization does not occur during the heating process was essentially the same for both ESD and FD preparations at PVP/PDN = 4/6. Thus, the solubility of PDN in the PVP matrix appears to be much higher than that of CBZ. Fig. 10 shows DSC curves after heating

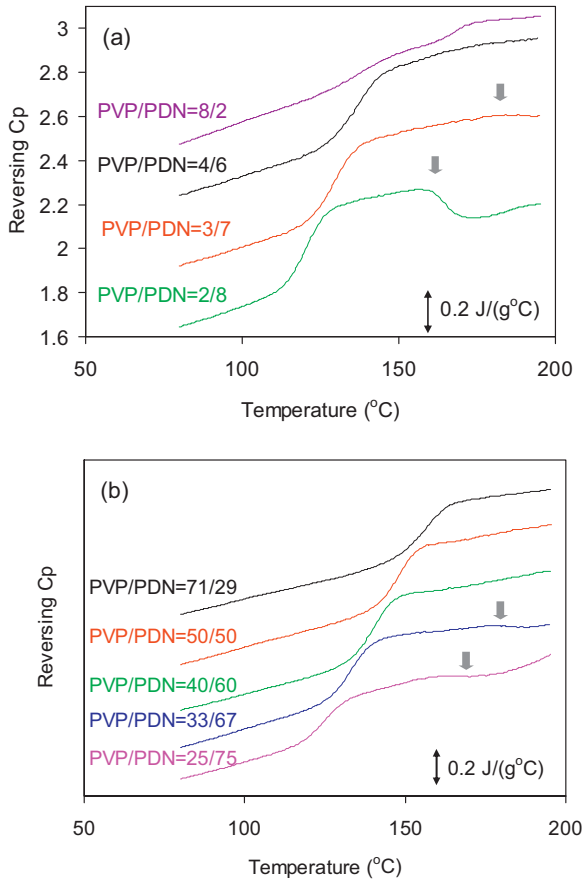

Fig. 10. Reversing heat capacity (Cp) for (a) FD and (b) ESD formulations prepared using PVP K90 and PDN. The mixing ratios are presented in the figure. The measurements were done after heating the sample up to 150 °C at 10 °C/min. The arrows indicate that crystallization endotherms were observed in the non-reversing heat flow at those temperatures.

up to 150 °C, which was found to be the optimum temperature for the removal of moisture without causing crystallization. In this case, modulated-temperature mode offered clearer DSC curves for observing the glass transition behavior. Reversing C_p is shown in the figure.

It is interesting to note that two glass transition temperatures were evident when PVP/PDN ratio was higher than 8/2 for the FD samples, while only one glass transition temperature appeared upon increase of the PDN content. This was not the case for the ESD samples; no phase separation was observed when the PDN content was low. This can be understood in terms of separation of the pure PVP phase. Although this does not cause a physical stability problem from a practical viewpoint, the formulation volume could be reduced because there is excess amount of PVP.

The crystallization heat flow cannot be observed in the reversing C_p; however, it can be reflected as a change in the heat capacity. The arrows in the Fig. 10 indicate that the crystallization exotherm was observed in the non-reversing heat flow at those points. Crystallization of PDN was observed when the PDN content was higher than PVP/PDN = 3/7 and 33/67 for the FD and ESD formulations, respectively. Thus, the loading limit appeared to be the same at ca. 60% for both preparation methods. In the combination of PVP and PDN, the only obvious difference in the mixing state was separation of pure PVP phase in the FD formulations, when PVP/PDN ratio was very high. Similarity in the structure for the both preparation methods may be explained in terms of relatively strong interaction between PVP and PDN that inhibits separation according to the molecular weight difference in the ESD process.

3.5. Difference between CBZ and PDN on interaction with PVP

In the ESD process, phase separation due to differences in the molecular weight is expected in addition to thermodynamic miscibility. SEM observation indicated that CBZ may fill the empty cores of the particles, while this was not the case for PDN. The higher thermodynamic miscibility of PDN with PVP was revealed by seminal DSC studies, so that the miscibility seemed to be an additional factor that influences the dynamic phase separation in the preparation process of ESD. In other words, phase separation due to the molecular weight difference could be hindered by the attractive interaction between PVP and PDN. Therefore, both thermodynamic and dynamic factors play important roles to determine the structure of the ESD particles.

The free energy of mixing can be described using the Flory–Huggins equation:

$$\frac{\Delta G_i}{kT} = \phi_d^i \ln \phi_d^i + \frac{\phi_p^i}{N} \ln \phi_p^i + \chi \phi_d^i \phi_p^i \quad (3)$$

where ΔG_i, ϕ_d^i, and ϕ_p^i are the mixing free energy, drug fraction, and polymer fraction of phase i, respectively. χ is the interaction parameter between the drug and polymer, for which a miscible combination provides a value less than 0.5, while a value greater than 0.5 indicates an immiscible combination. k and N are the Boltzmann constant and segment number of the polymer molecule, respectively. The overall mixing free energy ΔG can be written as

$$\Delta G = X_d \Delta G_d + X_p \Delta G_p \quad (4)$$

Subscripts d and p represent the drug-rich and polymer-rich phases, respectively, and X is the fraction of each phase. The equilibrium state results from the minimization of ΔG. Miscibility of the FD product should reflect the thermodynamic miscibility, because it can be formed slowly. Thus, a value of the χ parameter can be obtained for combinations of CBZ–PVP and PDN–PVP by minimizing Eq. (4) as 0.86 and 0.70, respectively, from the maximum loading values for the FD products.

The χ value can also be estimated by melting point depression analysis (Marsac et al., 2006, 2009). A trace amount of PVP K90 was added to CBZ and PDN to observe the melting behavior. In the case of CBZ, although quantitative analysis appeared to be difficult due to broadness of the melting peak even in the presence of very small amount of PVP (below 0.5%, w/w), it was obvious that the melting point was decreased upon addition of PVP. Thus, the χ value between PVP and CBZ can be regarded as negative at the melting temperature. In contrast, the melting point was increased upon addition of PVP to PDN. The melting enthalpy of PDN cannot be precisely determined, because its melting behavior overlaps with its degradation, and therefore the χ value between PVP and PDN cannot be determined. However, it was obvious that the χ value was positive at the melting temperature. It is interesting to note that the miscibility with PVP was better for CBZ at the melting temperature, although it was better for PDN in the case of the FD products. This observation indicates that the melting point depression analysis does not work for the prediction of miscibility for formulations prepared at lower temperatures.

3.6. Effect of thermal treatment on the formulation homogeneity

Heating of PVP–CBZ formulations up to above the melting temperature of CBZ produced a homogeneous amorphous structure. The miscibility is significantly dependent on the temperature; therefore, formation of the homogeneous structure should be due to high miscibility at that temperature, as indicated by the melting point depression study. This indicates the advantage of high-temperature processing to obtain homogeneous amorphous formulations. In this regard, hot-melt extrusion can be regarded

as a very powerful method to produce homogeneous formulations. A good example is presented by Guns et al., in which miconazole was loaded into poly (ethyleneglycol-co-vinyl alcohol) at 21% using hot-melt extrusion, while some crystallization was observed upon addition of 12% of the drug in the spray-drying product (Guns et al., 2011). However, it also means that formulations prepared at high temperature are in a very high-energy state when stored under ambient temperature conditions. Thus, much attention must be given to the time-dependent phase separation into drug-rich and polymer-rich phases to assure the physical stability of amorphous formulations.

3.7. Effect of the dynamic process during ESD on the particle structure

One of the most important indications obtained in this study is the spontaneous formation of core (drug)–shell (polymer) structure in the dried particles. However, it should be stressed that this assumption was made only by indirect evidences including clear phase separation in the ESD samples. Although preliminary X-ray photoelectron spectroscopy studies were performed to prove preferential accumulation of the polymer molecules on the surface in the ESD particles, quantitative reliability of the analysis was not high enough, because there were no specific atoms that help the analysis in the components used in this study. Nevertheless, this assumption can be supported by many earlier observations. Peclet number, *Pe*, is frequently used to explain this phenomenon (Vehring, 2008; Kawakami et al., 2010).

$$Pe = \frac{R_d^2}{\tau D_i} \quad (5)$$

where R_d, τ, D_i are the radius of the droplet, the drying time, and the diffusion coefficient of the component *i*, respectively. A large *Pe* means that the component cannot follow the shrinkage of the droplets, and thus the component is likely to accumulate on the surface region. If this is the case for all components included, then hollow particles are expected. On the other hand, a small *Pe* means that the diffusion of the component is sufficiently fast to follow the shrinkage of the droplets. Difference in the molecular weight of PVP K90 and the model drugs used in this study is more than three orders of magnitude, which results in huge difference in the diffusion coefficient. Thus, it seems to be natural to expect spontaneous phase separation due to the difference in the molecular weight. An important additional indication obtained in this study is that interaction between the components influences their dynamic separation process as well, because the phase separation of PVP–PDN was not significantly affected as the case for PVP–CBZ.

4. Conclusions

Particulate solid dispersions were prepared using electrospray deposition technology. In our previous electrospray deposition studies, productivity of the formulation was not practically realistic. Thus, productivity was increased by increasing the nozzle number used to prepare bulk formulations. Even in the scaled-up system, each solution and operation parameter, including solution concentration, conductivity, and flow rate, had the same effect on the particle formation. Therefore, the particle size could be reduced to nano-scale by increasing the conductivity of the solution through the addition of salts. When PVP K90 was used as an excipient, CBZ was homogeneously loaded up to ca. 40%, and with larger additions, the excess CBZ was separated as a pure crystalline phase. PDN was homogeneously loaded up to ca. 60%. However, in contrast to CBZ, the excess PDN maintained the amorphous state, even when a large amount was added. Both the thermodynamic and dynamic factors had a significant influence on the mixing state of each component in the ESD particles.

Acknowledgements

This work was supported by The Cosmetology Research Foundation and in part by World Premier International Research Center (WPI) Initiative on Materials Nanoarchitectonics, MEXT, Japan. Also acknowledged is Ms. Kyoko Iino for some assistance in the experiments.

References

Baird, J.A., van Eerdenbrugh, B., Taylor, L.S., 2010. A classification system to assess the crystallization tendency of organic molecules from undercooled melts. J. Pharm. Sci. 99, 3787–3806.
Bhugra, C., Pikal, M.J., 2008. Role of thermodynamic, molecular, and kinetic factors in crystallization from the amorphous state. J. Pharm. Sci. 97, 1329–1349.
Breitenbach, J., 2002. Melt extrusion: from process to drug delivery technology. Eur. J. Pharm. Biopharm. 54, 107–117.
Byrn, S.R., Xu, W., Newman, A.W., 2001. Chemical reactivity in solid-state pharmaceuticals: formulation implications. Adv. Drug Deliv. Rev. 48, 115–136.
Chakraborty, S., Liao I-Chien Adler, A., Leong, K.W., 2009. Electrohydrodynamics: a facile technique to fabricate drug delivery systems. Adv. Drug Deliv. Rev. 61, 1043–1054.
De Gennes, P.G., 2002. Solvent evaporation of spin cast films: crust effects. Eur. Phys. J. E 7, 31–34.
Ganán-Calvo, A.M., Dávila, J., Barrero, A., 1997. Current and droplet size in the electrospraying of liquids. Scaling laws. J. Aerosol Sci. 28, 249–275.
Grzesiak, A.L., Lang, M., Kim, K., Matzger, A.J., 2003. Comparison of the four anhydrous polymorphs of carbamazepine and the crystal structure of form I. J. Pharm. Sci. 92, 2260–2271.
Guns, S., Dereymaker, A., Kayaert, P., Mathot, V., Martens, J.A., Van den Mooter, G., 2011. Comparison between hot-melt extrusion and spray-drying for manufacturing solid dispersions of the graft copolymer of ethylene glycol and vinylalcohol. Pharm. Res. 28, 673–682.
Kawakami, K., 2009. Current status of amorphous formulation and other special dosage forms as formulations for early clinical phases. J. Pharm. Sci. 98, 2875–2885.
Kawakami, K., 2010. Parallel thermal analysis technology using an infrared camera for high-throughput evaluation of active pharmaceutical ingredients: a case study of melting point determination. AAPS PharmSciTech 11, 1202–1205.
Kawakami, K., Sumitani, C., Yoshihashi, Y., Yonemochi, E., Terada, K., 2010. Investigation of the dynamic process during spray-drying to improve aerodynamic performance of inhalation particles. Int. J. Pharm. 390, 250–259.
Kawakami, K., 2012. Modification of physicochemical characteristics of active pharmaceutical ingredients and application of supersaturatable dosage forms for improving bioavailability of poorly absorbed drugs. Adv. Drug Deliv. Rev. 64, 480–495.
Luthra, S.A., Hodge, I.M., Utz, M., Pikal, M.J., 2008. Correlation of annealing with chemical stability in lyophilized pharmaceutical glasses. J. Pharm. Sci. 97, 5240–5251.
Marsac, P.J., Shamblin, S.L., Taylor, L.S., 2006. Theroretical and practical approaches for prediction of drug–polymer miscibility and solubility. Pharm. Res. 23, 2417–2426.
Marsac, P.J., Li, T., Taylor, L.S., 2009. Estimation of drug–polymer miscibility and solubility in amorphous solid dispersions using experimentally determined interaction parameters. Pharm. Res. 26, 139–151.
Okuzono, T., Ozawa, K., Doi, M., 2006. Simple model of skin formation caused by solvent evaporation in polymer solutions. Phys. Rev. Lett. 97, 136103.
Serajuddin, A.T.M., 1999. Solid dispersion of poorly-soluble drugs: early promises, subsequent problems, and recent breakthroughs. J. Pharm. Sci. 88, 1058–1066.
Vehring, R., 2008. Phamaceutical particle engineering via spray drying. Pharm. Res. 25, 999–1022.
Zhang, S., Kawakami, K., 2010. One-step preparation of chitosan solid nanoparticles by electrospray deposition. Int. J. Pharm. 397, 211–217.
Zhang, S., Kawakami, K., Yamamoto, M., Masaoka, Y., Kataoka, M., Yamashita, S., Sakuma, S., 2011. Coaxial electrospray formulations for improving oral absorption of a poorly water-soluble drug. Mol. Pharm. 8, 807–813.